

Positron Lifetime Spectra in Molecular Gases*

P. E. OSMON†

Physics Department, Columbia University, New York, New York

(Received 12 May 1965)

Positron lifetime spectra have been measured in a wide variety of molecular gases at pressures up to about thirty atmospheres. The spectra were analyzed to yield the free-positron annihilation rate (λ_{e^+}) and triplet-positronium quenching rate (λ_q) at unit pressure. Attachment of the free positrons occurs in many of the gases. For the others, a strong correlation between λ_{e^+} and α , the electric-dipole polarizability at optical frequencies, is found, leading to a general relationship (for both molecular and atomic gases) between these two quantities. This is apparently the first experimental evidence that long-range dipole distortion is the predominant mechanism in low-energy positron scattering.

I. INTRODUCTION

POSITRON lifetime spectra have been measured in molecular gases at pressures up to about 30 atm.

It is generally believed¹⁻⁶ that the lifetime spectrum of positions released in a gas is a superposition of two exponentials:

$$I = I_1 \lambda_1 e^{-\lambda_1 t} + I_2 \lambda_2 e^{-\lambda_2 t}. \quad (1)$$

The first exponential describes the decay by annihilations of free positrons; the second, the decay of triplet positronium. The free-positron annihilation rate is pressure- (strictly, density-) proportional, and so we define $p\lambda_{e^+} = \lambda_1$, where p is the gas pressure. The pressure dependence of the positronium annihilation rate is given by

$$\lambda_2 = \lambda_0 + p\lambda_q, \quad (2)$$

where λ_0 is the natural annihilation rate of 1^3S positronium ($7.20 \mu\text{sec}^{-1}$)⁷ and λ_q is the quenching rate per unit pressure.

However, recent measurements of lifetime spectra in the noble gases⁸⁻¹¹ contradict this simple picture: A distinct plateau is observed commencing close to time zero, and only after this plateau is the expected shape of Eq. (1) observed.

The plateau has been associated with moderation of the free positrons in the range: threshold for inelastic collisions (≈ 10 eV for noble gases) down to thermal equilibrium. Thus a measurement of the width of the

plateau is an indirect measure of the positron-atom elastic-collision cross section (strictly, momentum-transfer cross section) over this energy range. This picture has been confirmed by the observation⁸ that the plateau width is reduced, in the case of argon, by contaminating with nitrogen, the low-lying molecular energy levels permitting inelastic (and therefore rapid) energy loss by the positron right down to thermal energy. Recent measurements⁶ of lifetime spectra in propane and other vapors, where no plateaus were reported, also support this picture.

Where a plateau is observed, the origin of the pressure-proportional first exponential of Eq. (1) is not obvious. One possibility¹¹ is that this describes loss of positrons from the distribution by attachment to gas molecules.

It has seemed desirable, for several reasons, to examine the lifetime spectra of positrons in a wide variety of molecular gases: first, to search for plateaus, or other departures from the spectrum of Eq. (1) to test the general correctness of our new picture of slow-positron behavior; second, although positron collision and annihilation processes in molecular gases are sufficiently complicated that detailed calculations are hardly possible, the usefulness of mixtures containing these for unfolding details of noble-gas spectra calls for at least approximate knowledge of their spectra; third, to try to determine the physical effects dominating slow-positron collisions. The possibilities include long-range polarization of the atom, virtual positronium formation during the collision, as well as virtual and real attachment of the positron.

II. METHOD

The apparatus has already been described.¹¹ A 100-Mc/sec digitron of near-perfect differential linearity was used for absolute calibration of the time scale. The method consisted in measuring the decay rate of the same single-component positron-lifetime spectrum with first the time-amplitude converter and then the digitron. The raw spectra were taken from the 512-channel analyzer and fed into the Columbia University 7090 computer where they were corrected for nonlinearity of the time scale, and the random-coincidence back-

* Work supported in part by the U. S. Atomic Energy Commission.

† Present address: Physics Department, Westfield College, London University, London, England.

¹ M. Deutsch, *Progr. Nucl. Phys.* **3**, 131 (1953).

² G. M. Lewis and A. T. G. Ferguson, *Phil. Mag.* **44**, 1011 (1963).

³ T. B. Daniel and R. Stump, *Phys. Rev.* **115**, 1599 (1959).

⁴ F. F. Heymann, P. E. Osmon, J. J. Veit, and W. F. Williams, *Proc. Phys. Soc. (London)* **A78**, 1039 (1961).

⁵ B. G. Duff and F. F. Heymann, *Proc. Roy. Soc. (London)* **A270**, 517 (1963).

⁶ D. A. Paul and L. Saint Pierre, *Phys. Rev. Letters* **11**, 493 (1963).

⁷ A. Ore and J. L. Powell, *Phys. Rev.* **75**, 1696 (1949).

⁸ S. J. Tao, J. Bell, and J. H. Green, *Proc. Phys. Soc. (London)* **83**, 453 (1964).

⁹ W. R. Falk and G. Jones, *Can. J. Phys.* **42**, 1751 (1964).

¹⁰ D. A. L. Paul, *Proc. Phys. Soc. (London)* **84**, 563 (1964).

¹¹ P. E. Osmon, *Phys. Rev.* **138**, B216 (1965).

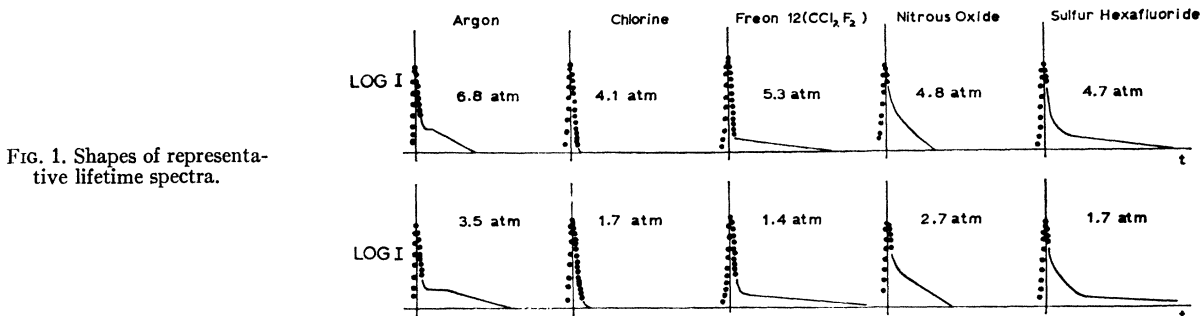


FIG. 1. Shapes of representative lifetime spectra.

ground was subtracted. The resulting "pure" spectra were plotted and the region clear of the prompt peak was fitted to a sum of two exponentials according to Eq. (1). The peak was subtracted together with the background using a "chamber empty" spectrum. A difficulty was encountered here. Because the counting rate in peak channels was about three orders of magnitude greater than in a typical channel away from the peak, the base of the prompt peak was feeding through into the delayed region of the time spectrum, and small drifts prevented complete subtraction. For this reason the curve fitting was halted 30 nsec from the peak.

III. SPECTRA

The shapes of representative lifetime spectra are shown in Fig. 1. Including two argon spectra for comparison. Background has been subtracted, but the prompt peaks retained. The decay rates of the exponentials have been measured, and by examining the pressure dependence have been associated with free or with positronium annihilations according to Eq. (2). The results are displayed in the table. For many gases, one or both of the decay rates was apparently missing. However, in these cases the prompt peaks were not completely symmetrical about time zero, and the peak widths decreased with pressure. Evidently the annihilation rates were too great to be measured by the present apparatus. These spectra are being reexamined at higher resolution and dispersion.

In two gases, nitrogen and nitrous oxide, a region of the spectrum has a definite concavity towards the time axis, but unlike the case of the noble gases no actual plateaus have been observed.

IV. DISCUSSION

In contrast with the situation in the noble gases, because of the existence of molecular levels right down through thermal energy, we may assume the positron has reached thermal equilibrium with the gas after the first few nanosecond atmospheres of its lifetime. An inspection of Table I immediately suggests a division of the annihilation processes, free and bound, into the two categories: rapid and slow.

Rapid annihilations of triplet positronium in nitric oxide, nitrogen dioxide, chlorine, and oxygen were dis-

covered by Deutsch¹ who has also investigated the possible quenching mechanisms. Sulfur dioxide now joins the group. However, the nature of its quenching mechanism is not obvious.

Slow annihilations of positronium occur universally⁴ through the mechanism of pickoff quenching whereby the positron annihilates with an atomic electron during a collision. Figure 2 shows some correlation of pickoff quenching rate λ_q with the number of atomic electrons (λ_{Dirac}). The behavior of nitrous oxide is anomalous.

Rapid annihilations of free positrons were previously observed by Deutsch¹ and Lewis and Ferguson² in Freon 12. More recently they have been observed in a range of gases by Paul and Saint Pierre.⁶ The likely mechanism is attachment of the positron to a gas molecule, with a large cross section for this process below some threshold, probably at around thermal energy.

Slow annihilation of free positrons is the process one is most hopeful of learning about from the present data. Positrons with velocity substantially greater than the orbital velocity of the molecular electrons see an aver-

TABLE I. Comparison of measured rates with Dirac rate. For each gas, spectra were measured at about four pressures over the range zero to the maximum pressure listed.

Gas	Maximum pressure (atm)	λ_{e^+} ($\mu\text{sec}^{-1} \text{atm}^{-1}$)	λ_q ($\mu\text{sec}^{-1} \text{atm}^{-1}$)	λ_{Dirac} ($\mu\text{sec}^{-1} \text{atm}^{-1}$)
H ₂	34.3	2.15±0.15	0.08±0.03	0.4
H ₂ S	4.9	>100	0.72±0.15	1.8
NH ₃	4.4	>100	0.43±0.15	2.0
N ₂	34.8	3.95±1.0	0.21±0.10	2.8
NO	3.4	>200	>200	3.0
O ₂	34.9	3.6±0.3	>60	3.2
HCl	9.9	>100	0.52±0.11	3.6
CBF ₃	10.4	>60	0.71±0.15	3.8
HCClF ₂	9.2	>150	0.31±0.07	4.2
CO ₂	17.1	4.5±1.5	0.27±0.15	4.4
N ₂ O	8.9	>100	8.6±0.5	4.4
NO ₂	3.0	>300	>300	4.6
CCl ₂ F ₂	5.3	>100	0.29±0.07	5.8
CF ₂ =CH ₂	16.7	7.8±3.0	0.30±0.13	6.4
SO ₂	2.2	>70	>70	6.4
CHF ₃	22.9	8.9±3.0	0.25±0.08	6.8
Cl ₂	4.1	>200	>200	6.8
C ₂ ClF ₆	6.2	>60	0.49±0.15	7.4
CF ₄	17.4	4.8±1.0	0.27±0.07	8.4
CClF ₃	18.3	13.8±4.0	0.31±0.03	10.0
SF ₆	4.7	37.8±8.0	1.32±0.30	14.0

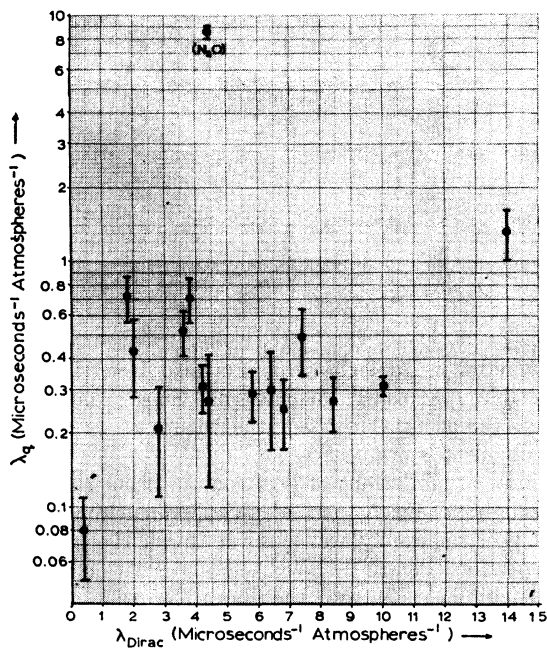


FIG. 2. Slow positronium annihilation rates versus the Dirac rates.

age electron density in their path

$$\rho = pLz,$$

where p is the gas pressure in atmospheres, L is Loschmidt's number, and z is the number of electrons

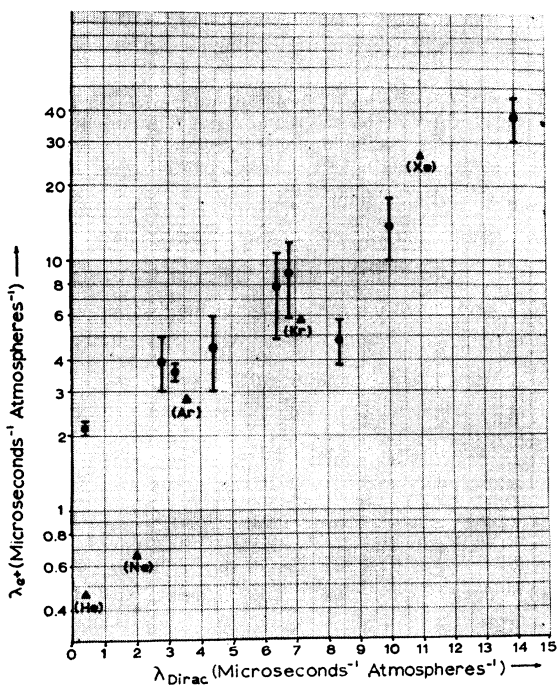


FIG. 3. Slow free-positron annihilation rates versus the Dirac rates.

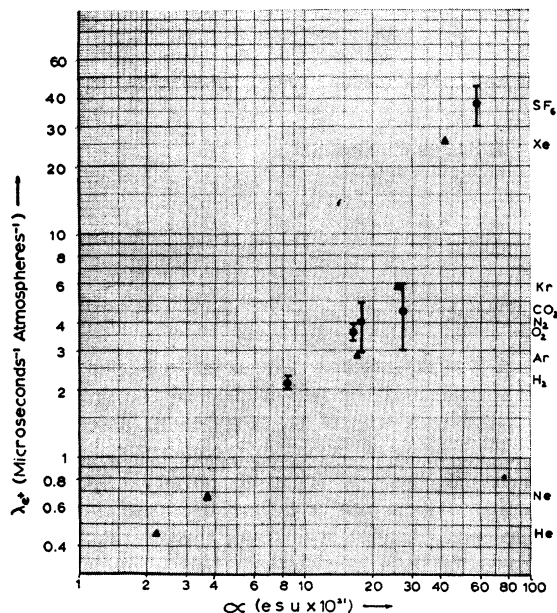


FIG. 4. Slow free-positron annihilation rates versus electric-dipole polarizabilities.

per molecule. The so-called Dirac rate is defined to be

$$\lambda_{\text{Dirac}} = \pi r_0^2 c LZ.$$

A lower energy positron should be repelled by the atomic field and so see an electron density much smaller than this. But in fact, with the single exception of CF_4 , we observe

$$\lambda_{e^+} > \lambda_{\text{Dirac}}.$$

So the positron has somehow to distort the atomic field so that the local electron density is enhanced.

As a positron approaches a gas atom from a great distance, the first interaction between them has the potential

$$U = -e^2\alpha/r^4,$$

where α is the polarizability of the atom. The approaching positron has induced a dipole moment in the atom. This long-range interaction is one possible mechanism for enhancing the annihilation rate.

Short-range distortions are also possible. They may be described by virtual excitation of higher electronic states of the molecule, formation of virtual positronium, or formation of a virtual positron-molecule complex.

Figure 3 shows λ_{e^+} plotted versus λ_{Dirac} for the slow annihilating gases (including data for the noble gases taken from Ref. 8). There is evidently a correlation between λ_{e^+} and λ_{Dirac} . And for the molecular gases a smooth curve can be drawn through the points. The noble atoms however are notably less effective annihilators. Presumably they distort less easily.

In Fig. 4 λ_{e^+} is plotted versus α , the polarizability,

determined from refractivity. (A thermal positron has a velocity of about 10^7 cm sec $^{-1}$, so that for a molecule of dimension about 10^{-7} to 10^{-8} cm the passing positron looks like a transitory alternating electric field of frequency 10^{14} to 10^{15} sec $^{-1}$ i.e., the frequency of visible light.)

The correlation of λ_{e^+} with α is evidently much stronger than with λ_{Dirac} . In fact from Fig. 4 we can get approximately,

$$\lambda_{e^+} = \alpha^{1.25}/10$$

for all gases, with λ_{e^+} in $\mu\text{sec}^{-1} \text{ atm}^{-1}$, α in esu $\times 10^{21}$.

This general relationship seems to demonstrate that the long-range dipole distortion is the predominant mechanism in low-energy positron scattering. This has not previously been clear, either in the positron case, or for slow-electron collisions. There is support for this picture from recent calculations of Cody *et al.*¹²

¹² W. J. Cody, Joan Lawson, Sir Harrie Massey, and K. Smith, Proc. Roy. Soc. (London) **A278**, 479 (1964).

The Transition $1s\sigma_g - 2p\sigma_u$ in H_2^+ Induced by Collision with an Electron, Proton, or Hydrogen Atom*

JAMES M. PEEK

Sandia Laboratory, Albuquerque, New Mexico

(Received 12 April 1965)

The first Born approximation to the transition $1s\sigma_g - 2p\sigma_u$ in H_2^+ is developed. The internal degrees of freedom of the molecular ion are treated explicitly, and in a manner that takes advantage of the dissociative nature of the $2p\sigma_u$ state. The resulting total cross section is found to depend on the initial vibrational state. Numerical results are presented in graphical form for the cases in which this process is caused by collision with an electron, proton, or hydrogen atom. In each case the total cross section is given for all 19 bound vibrational states of the H_2^+ ground state (the $1s\sigma_g$ orbital). In the electron and proton cases the cross section for the lowest ($\nu=0$) vibrational state is observed to be two orders of magnitude lower than the cross section for the last ($\nu=18$) bound vibrational state. The dependence on initial vibrational state in the hydrogen-atom case is not as dramatic as in the bare-charge cases, but simultaneous excitation of the hydrogen atom is demonstrated to be an important factor in the shape and magnitude of the cross section. A method of summing simultaneous excitations is presented for the situation in which one particle undergoes a specific transition and the other particle is left in an unspecified state.

I. INTRODUCTION

PREVIOUS theoretical treatments^{1,2} of scattering by the hydrogen-molecule ion H_2^+ indicate that the internal degrees of freedom of this molecular ion must be considered to predict its scattering behavior accurately. This is particularly true because the major mechanism leading to the formation of H_2^+ is $\text{H}_2(1\Sigma_g^+) \rightarrow \text{H}_2^+(2\Sigma_g^+) + e^-$, where the Franck-Condon factors predict a finite probability of occupation³ of all bound vibrational states of the $2\Sigma_g^+$ electronic state. These states also have long lifetimes, because they must decay by a quadrupole mechanism; hence any experiment performed with H_2^+ could easily involve all 19 bound vibrational states.⁴

In this paper we investigate the total cross section for the inelastic process

$$a + \text{H}_2^+(1s\sigma_g) = a + \text{H}_2^+(2p\sigma_u), \quad (1)$$

* This work was supported by the U. S. Atomic Energy Commission.

¹ James M. Peek, Phys. Rev. **134**, A877 (1964).

² E. H. Kerner, Phys. Rev. **92**, 1441 (1953).

³ J. Wm. McGowan and L. Kerwin, Can. J. Phys. **42**, 972 (1964).

⁴ S. Cohen, J. R. Hiskes, and R. J. Riddell, Jr., Phys. Rev. **119**, 1025 (1960).

where each bound vibrational state of $\text{H}_2^+(1s\sigma_g)$ is considered separately and a is an electron, proton, or hydrogen atom. The orbital designating the electronic eigenstate of H_2^+ is given in parentheses. It will then be possible, with a knowledge of the population of vibrational states, to predict an observed cross section by forming the appropriate average of the results for the individual vibrational states.⁵ Investigation of transitions to several lower lying electronic states¹ has shown that the reaction indicated by Eq. (1), in the electron case, dominates the discrete transitions proceeding from the ground state. The $2p\sigma_u$ state has no bound vibrational states; hence, in the electron or proton case, the cross sections given here will be good approximations to the dissociation process that results in a proton and hydrogen atom.

The approach will be that of Ref. 1 (to be referred to as I); that is, the total cross section will be calculated in the first Born approximation and it will include the contributions from all eigenstates of nuclear motion for the final electronic configuration. The method used in I for summing the contributions from all final eigenstates of

⁵ See Eq. (13).

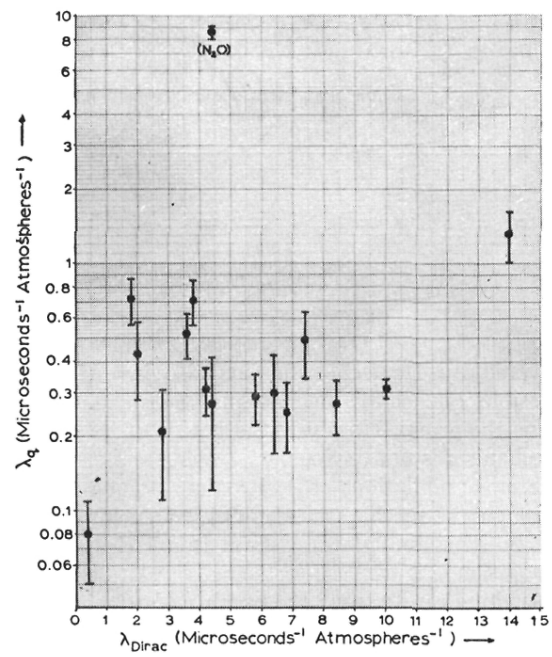


FIG. 2. Slow positronium annihilation rates versus the Dirac rates.

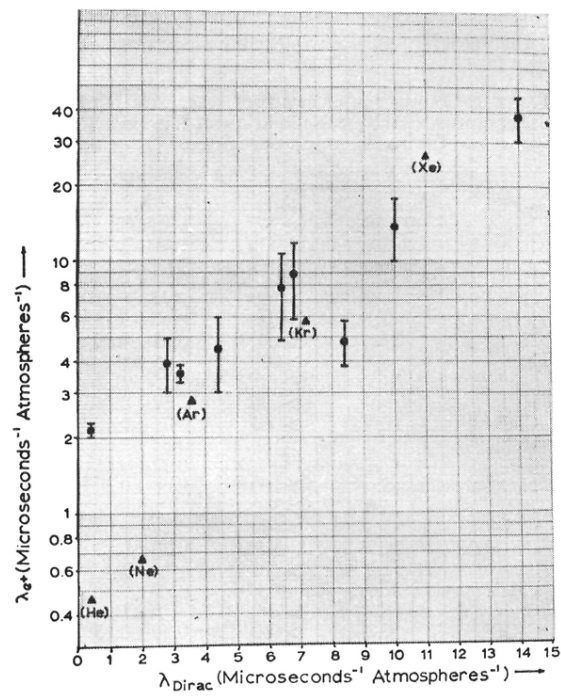


FIG. 3. Slow free-positron annihilation rates versus the Dirac rates.

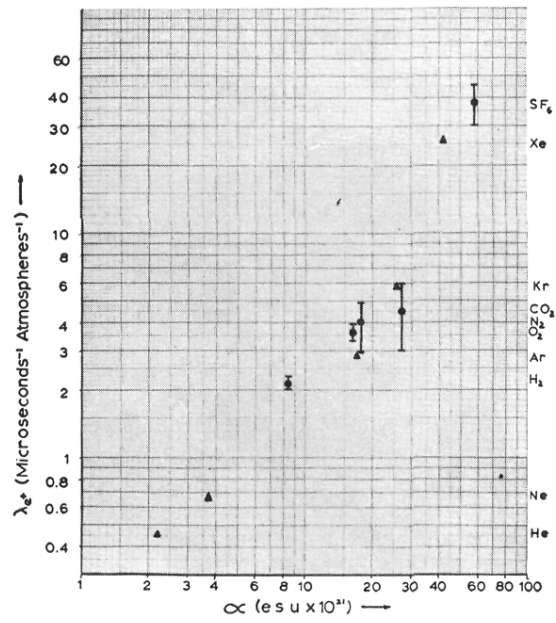


FIG. 4. Slow free-positron annihilation rates versus electric-dipole polarizabilities.